Einstein-Podolsky-Rosen-steering swapping between two Gaussian multipartite entangled states

Meihong Wang,[1] Zhongzhong Qin,[1,2] Yu Wang,[3,*] and Xiaolong Su[1,2,†]

[1]*State Key Laboratory of Quantum Optics and Quantum Optics Devices, Institute of Opto-Electronics, Shanxi University, Taiyuan 030006, China*
[2]*Collaborative Innovation Center of Extreme Optics, Shanxi University, Taiyuan 030006, China*
[3]*State Key Laboratory of Cryptology, Beijing 100878, China*
(Received 22 June 2017; published 7 August 2017)

Multipartite Einstein-Podolsky-Rosen (EPR) steering is a useful quantum resource for quantum communication in quantum networks. It has potential applications in secure quantum communication, such as one-sided device-independent quantum key distribution and quantum secret sharing. By distributing optical modes of a multipartite entangled state to space-separated quantum nodes, a local quantum network can be established. Based on the existing multipartite EPR steering in a local quantum network, secure quantum communication protocol can be accomplished. In this manuscript, we present swapping schemes for EPR steering between two space-separated Gaussian multipartite entangled states, which can be used to connect two space-separated quantum networks. Two swapping schemes, including the swapping between a tripartite Greenberger-Horne-Zeilinger (GHZ) entangled state and an EPR entangled state and that between two tripartite GHZ entangled states, are analyzed. Various types of EPR steering are presented after the swapping of two space-separated independent multipartite entanglement states without direct interaction, which can be used to implement quantum communication between two quantum networks. The presented schemes provide technical reference for more complicated quantum networks with EPR steering.

I. INTRODUCTION

A local quantum network can be established by distributing optical modes of a multipartite entangled state to space-separated quantum nodes. By connecting several space-separated local quantum networks, a global quantum network can be established. It has been experimentally demonstrated that a feasible method to connect two multipartite entangled states (two local quantum networks) is by using entanglement swapping [1]. Entanglement swapping [2–7], which makes two independent quantum entangled states without direct interaction become entangled, is an important technique in building a quantum information network [8,9]. Entanglement swapping has been experimentally demonstrated in both discrete and continuous variables regions [10,11], and between discrete and continuous variable systems [12]. The entanglement swapping among three two-photon Einstein-Podolsky-Rosen (EPR) entangled states has been used to generate a Greenberger-Horne-Zeilinger (GHZ) state [13]. The technique of entanglement swapping has been applied to complete remote transfer of Gaussian quantum discord [14]. Recently, the quantum entanglement swapping between two multipartite entangled states has been demonstrated experimentally [1], which shows the feasibility of connecting two multipartite entangled states by entanglement swapping.

Besides quantum entanglement, EPR steering is another kind of quantum resource for quantum information [15–17]. Suppose Alice and Bob share an EPR entangled state and they are separated in space. EPR steering means that one party, say Alice, can "steer" the state in Bob's station by performing measurements on her state at a distance, i.e., if Alice makes a measurement on her state, the state in Bob's station will change

instantaneously. In the hierarchy of quantum correlations, EPR steering represents a weaker form of quantum nonlocality and stands between Bell nonlocality [18] and EPR entanglement [19]. Concretely, violation of Bell inequality implies EPR steering in both directions, and EPR steering of any direction implies that the quantum state is entangled [20].

EPR steering has recently attracted increasing interest in quantum optics and quantum information communities [20–22]. Different from entanglement and Bell nonlocality, the asymmetric feature is a unique property of EPR steering [20,23–26]. EPR steering can be regarded as verifiable entanglement distribution by an untrusted party, while entangled states need both parties to trust each other, and Bell nonlocality is valid assuming that they distrust each other [21]. In the field of quantum information processing, EPR steering has potential applications in one-sided device-independent quantum key distribution [27], quantum secret sharing (QSS) [28], channel discrimination [29] and secure quantum teleportation [30,31]. Very recently, the Gaussian quantum-steering swapping between two EPR entangled states has been analyzed theoretically [32], which provides a technical reference for remote quantum communications with EPR steering. It has also been experimentally demonstrated that the direction of one-way EPR steering can be actively manipulated [33], which may lead to more consideration in the application of EPR steering. The investigation of EPR steering has also been extended to the multipartite state. Experimental observation of multipartite EPR steering has been reported in optical networks [24] and photonic qubits [34,35]. Interestingly, EPR steering in the multipartite state is limited by the so-called monogamy relations [28,36–39]. Very recently, the monogamy relations for EPR steering in a Gaussian cluster state has been demonstrated experimentally [40].

Based on the existence of multipartite EPR steering in a local quantum network, secure QSS protocol can be

*sxuwy@hotmail.com
†suxl@sxu.edu.cn

accomplished [28]. If the users belong to two space-separated local quantum networks, how can they implement the QSS? A feasible method is implementing the QSS on a merged quantum network, which merges two local quantum networks into a larger quantum network. Based on the scheme introduced in Ref. [1], two multipartite entangled states can be merged into a larger multipartite entangled state by entanglement swapping. Then, the question is whether multipartite EPR steering still exists after the swapping operation.

In this paper, we present the swapping of EPR steering between two multipartite entangled states, which provides a feasible way to accomplish secure quantum communication protocols between two local quantum networks. Based on whether the number of quantum modes of two multipartite entangled states are the same or different, the swapping occurs between two symmetric or asymmetric multipartite entangled states. As examples, EPR steering in two swapping schemes, one between a tripartite Gaussian GHZ state and an EPR state (swapping scheme I) and one between two tripartite Gaussian GHZ states (swapping scheme II), are analyzed. In the swapping procedure, the optimal gain in the classical channel is used to optimize the output EPR steering. Various types of EPR steering are presented after the swapping, which can be used to implement different quantum communication protocols. The results for multipartite EPR steering are useful to multiparty quantum communication protocols [41,42] and are not guaranteed by multipartite entanglement.

II. EPR-STEERING SWAPPING SCHEMES

Suppose two space-separated multipartite entangled states A and B, consisting of m ($m \geqslant 2$) and n ($n \geqslant 2$) optical modes, respectively, are used to construct two local quantum networks A and B. To establish EPR steering between them, one optical mode from multipartite state A is sent to the multipartite entangled state B through a quantum channel. A joint measurement (usually a Bell state measurement) is implemented on the optical mode from multipartite state A and an optical mode from multipartite entangled state B and the measurement results are fed forward to the remaining optical modes of state B [1]. After the swapping operation, a new multipartite entangled state consisting of $m + n - 2$ modes will be obtained.

Figure 1 shows the schematic of two swapping schemes. The swapping between a tripartite GHZ state and an EPR state (swapping scheme I) and that between two tripartite GHZ states (swapping scheme II) are shown in Figs. 1(a) and 1(b), respectively. One of the optical modes located in network A is sent to one station of local network B through a quantum channel. A joint measurement is implemented in the station on the received optical mode and one of its optical modes [$\hat{E}_1$ in Fig. 1(a) and $\hat{B}_1$ in Fig. 1(b)] by coupling them on a 1:1 beam splitter. The output optical modes of the beam splitter are measured by two homodyne detectors and the measurement results are fed forward to the remaining optical modes of network B [$\hat{E}_2$ in Fig. 1(a) and $\hat{B}_2$ and $\hat{B}_3$ in Fig. 1(b)] through the classical channel, respectively. Different from the traditional entanglement swapping between two EPR entangled states, the feed-forward schemes of measurement results in the classical channels are more complex and depend
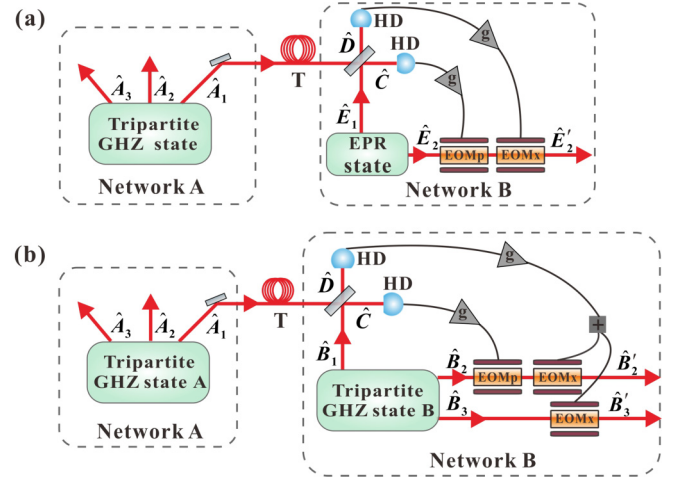

FIG. 1. Schematic of two multipartite steering swapping schemes. Networks A and B consist of two multipartite entangled states. A joint measurement is performed at local quantum network B and the measurement results are fed forward to the remaining modes of network B by classical channels. (a) Scheme for Gaussian EPR-steering swapping between a tripartite GHZ state and an EPR entangled state. (b) Scheme for Gaussian EPR-steering swapping between two tripartite GHZ entangled states. HD: homodyne detector; EOMp and EOMx: phase and amplitude electro-optical modulators; T: transmission efficiencies of the quantum channels.

on the types of quantum correlation between two multipartite entangled states.

The properties of a (n_A and m_B)-mode Gaussian state of a bipartite system can be determined by its covariance matrix

$$\sigma_{AB} = \begin{pmatrix} A & C \\ C^{\top} & B \end{pmatrix}, \qquad (1)$$

with matrix element $\sigma_{ij} = \langle \hat{\xi}_i \hat{\xi}_j + \hat{\xi}_j \hat{\xi}_i \rangle / 2 - \langle \hat{\xi}_i \rangle \langle \hat{\xi}_j \rangle$, where} $\hat{\xi} \equiv (\hat{x}_1^A, \hat{p}_1^A, \dots, \hat{x}_n^A, \hat{p}_n^A, \hat{x}_1^B, \hat{p}_1^B, \dots, \hat{x}_m^B, \hat{p}_m^B)$ is the vector of the amplitude and phase quadratures of optical modes. The submatrices A and B correspond to the reduced states of Alice's and Bob's subsystems, respectively.

The steerability of Bob by Alice [$\mathcal{G}^{A \to B}(\sigma_{AB})$] for a ($n_A + m_B$)-mode Gaussian state can be quantified by [43]

$$\mathcal{G}^{A \to B}(\sigma_{AB}) = \max \left\{ 0, \ -\sum_{j : \bar{v}_j^{AB \backslash A} < 1} \ln \left(\bar{v}_j^{AB \backslash A} \right) \right\}, \qquad (2)$$

where $\bar{v}_j^{AB \backslash A}$ ($j = 1, \dots, m_B$) are the symplectic eigenvalues of $\bar{\sigma}_{AB \backslash A} = B - C^{\top} A^{-1} C$, derived from the Schur complement of A in the covariance matrix σ_{AB}. The steerability of Alice by Bob [$\mathcal{G}^{B \to A}(\sigma_{AB})$] can be obtained by swapping the roles of A and B.

A. Steering swapping scheme I

In steering swapping between a tripartite GHZ state and an EPR state, shown in Fig. 1(a), the tripartite GHZ state located in network A is prepared by coupling a phase-squeezed state ($\hat{a}_2$) and two amplitude-squeezed states ($\hat{a}_1$ and $\hat{a}_3$) on an optical beam-splitter network, which consists of two optical beam splitters with transmissivity of $T_{A_1} = 1/3$ and $T_{A_2} = 1/2$ [1].

Three input squeezed states are expressed by

$$\hat{a}_1 = \tfrac{1}{2}\big(e^{-r_1}\hat{x}_1^{(0)} + ie^{r_1}\hat{p}_1^{(0)}\big),$$
$$\hat{a}_2 = \tfrac{1}{2}\big(e^{r_2}\hat{x}_2^{(0)} + ie^{-r_2}\hat{p}_2^{(0)}\big), \qquad (3)$$
$$\hat{a}_3 = \tfrac{1}{2}\big(e^{-r_3}\hat{x}_3^{(0)} + ie^{r_3}\hat{p}_3^{(0)}\big),$$

where r_i ($i = 1,2,3$) is the squeezing parameter, $\hat{x} = \hat{a} + \hat{a}^\dagger$ and $\hat{p} = (\hat{a} - \hat{a}^\dagger)/i$ are the amplitude and phase quadratures of an optical field $\hat{a}$, respectively, and the superscripts of the amplitude and phase quadratures represent the vacuum state. Under this notation, the variances of amplitude and phase quadratures for vacuum state are $V(\hat{x}_0) = V(\hat{p}_0) = 1$. The optical modes of the tripartite GHZ state in local network A are given by

$$\hat{A}_1 = \sqrt{\frac{2}{3}}\hat{a}_1 + \sqrt{\frac{1}{3}}\hat{a}_2, \qquad (4)$$

$$\hat{A}_2 = -\sqrt{\frac{1}{6}}\hat{a}_1 + \sqrt{\frac{1}{3}}\hat{a}_2 + \sqrt{\frac{1}{2}}\hat{a}_3,$$
$$\hat{A}_3 = -\sqrt{\frac{1}{6}}\hat{a}_1 + \sqrt{\frac{1}{3}}\hat{a}_2 - \sqrt{\frac{1}{2}}\hat{a}_3. \qquad (5)$$

The EPR entangled state located in network B is prepared by coupling a phase-squeezed state $[\hat{e}_1 = \tfrac{1}{2}(e^{r_1}\hat{x}_1^{(0)} + ie^{-r_1}\hat{p}_1^{(0)})]$ and a amplitude-squeezed state $[\hat{e}_2 = \tfrac{1}{2}(e^{-r_2}\hat{x}_2^{(0)} + ie^{r_2}\hat{p}_2^{(0)})]$ on a beam-splitter with transmissivity of $T_E = 1/2$ [1]. The optical modes of the EPR entangled state are expressed by

$$\hat{E}_1 = \sqrt{\frac{1}{2}}(\hat{e}_1 + \hat{e}_2),$$

$$\hat{E}_2 = \sqrt{\frac{1}{2}}(\hat{e}_1 - \hat{e}_2). \qquad (6)$$

The quantum correlations between the amplitude and phase quadratures of a tripartite entangled state and EPR entangled state are $\Delta^2(\hat{x}_{A_1} - \hat{x}_{A_2}) = \Delta^2(\hat{x}_{A_2} - \hat{x}_{A_3}) = \Delta^2(\hat{x}_{A_1} - \hat{x}_{A_3}) = 2e^{-2r}$, $\Delta^2(\hat{p}_{A_1} + \hat{p}_{A_2} + \hat{p}_{A_3}) = 3e^{-2r}$, and $\Delta^2(\hat{x}_{E_1} - \hat{x}_{E_2}) = \Delta^2(\hat{p}_{E_1} + \hat{p}_{E_2}) = 2e^{-2r}$, respectively. Here we assume that the squeezing parameters of all the squeezed states are equal.

Loss in quantum channels can lead to decoherence of a quantum state. Especially, the excess noise in a quantum channel can lead to the disappearance of squeezing and sudden death of entanglement [44,45]. Here we consider the case where the optical mode $\hat{A}_1$ is transmitted in a lossy channel. After being transmitted through a lossy channel, the optical mode $\hat{A}_1$ turns into $\hat{A}'_1 = \sqrt{T}\hat{A}_1 + \sqrt{1-T}\hat{v}$, where T and $\hat{v}$ represent the transmission efficiency of quantum channel and vacuum mode induced by loss into the quantum channel, respectively.

The optical modes $\hat{A}'_1$ and $\hat{E}_1$ are coupled on a 1:1 beam splitter and the output modes are $\hat{C} = (\hat{A}'_1 + \hat{E}_1)/\sqrt{2}$ and $\hat{D} = (\hat{A}'_1 - \hat{E}_1)/\sqrt{2}$, respectively. The phase quadrature of optical mode $\hat{C}$ $[\hat{p}_C = (\hat{p}_{A'_1} + \hat{p}_{E_1})/\sqrt{2}]$ and amplitude quadrature of optical mode $\hat{D}$ $[\hat{x}_D = (\hat{x}_{A'_1} - \hat{x}_{E_1})/\sqrt{2}]$ are measured by two homodyne detectors (HDs), respectively. The measurement results are fed forward to the mode $\hat{E}_2$ through classical channels. The phase-space displacement on

mode $\hat{E}_2$ is performed in network B with amplitude and phase modulators (EOMx and EOMp), respectively. The output beam is given by

$$\hat{E}'_2 = \hat{E}_2 + \sqrt{2}g\,\hat{x}_D + i\sqrt{2}g\,\hat{p}_C, \qquad (7)$$

where g describes the amplitude and phase gain factor in the classical channels; here we have assumed that the gains in two classical channels are equal. Finally, a tripartite state consisting of $\hat{A}_3, \hat{A}_2$, and $\hat{E}'_2$ is established. Based on the expressions of $\hat{A}_2$, $\hat{A}_3$, and $\hat{E}'_2$, the covariance matrix of the output tripartite state can be obtained and the existing EPR steering of output modes is verified.

B. Steering swapping scheme II

In steering swapping between two Gaussian tripartite GHZ states, shown in Fig. 1(b), the tripartite GHZ state in network A is the same as that in scheme I. The other tripartite GHZ state located in network B in scheme II is prepared by coupling a amplitude-squeezed state ($\hat{b}_3$) and two phase-squeezed states ($\hat{b}_1$ and $\hat{b}_2$) on an optical beam-splitter network, which consists of two optical beam splitters with transmissivity of $T_{B_1} = 1/3$ and $T_{B_2} = 1/2$ [1]. The optical modes of the tripartite GHZ state located in network B are given by

$$\hat{B}_1 = i\sqrt{\frac{2}{3}}\hat{b}_1 + \sqrt{\frac{1}{3}}\hat{b}_2,$$

$$\hat{B}_2 = -i\sqrt{\frac{1}{6}}\hat{b}_1 + \sqrt{\frac{1}{3}}\hat{b}_2 + \sqrt{\frac{1}{2}}\hat{b}_3, \qquad (8)$$

$$\hat{B}_3 = -i\sqrt{\frac{1}{6}}\hat{b}_1 + \sqrt{\frac{1}{3}}\hat{b}_2 - \sqrt{\frac{1}{2}}\hat{b}_3.$$

The quantum correlations between the amplitude and phase quadratures of two tripartite GHZ entangled states are $\Delta^2(\hat{x}_{B_1} - \hat{x}_{B_2}) = \Delta^2(\hat{x}_{B_2} - \hat{x}_{B_3}) = \Delta^2(\hat{x}_{B_1} - \hat{x}_{B_3}) = 2e^{-2r}$, and $\Delta^2(\hat{p}_{B_1} + \hat{p}_{B_2} + \hat{p}_{B_3}) = 3e^{-2r}$, respectively. Similarly, we assume that the squeezed parameters of all the squeezed states are equal.

In steering swapping scheme II, the joint measurement is implemented between optical modes $\hat{A}'_1$ and $\hat{B}_1$, which are coupled on a 1:1 beam splitter and the output modes are $\hat{C} = (\hat{A}'_1 + \hat{B}_1)/\sqrt{2}$ and $\hat{D} = (\hat{A}'_1 - \hat{B}_1)/\sqrt{2}$, respectively. The measured phase and amplitude quadratures of optical modes $\hat{C}$ and $\hat{D}$ are represented by $\hat{p}_C = (\hat{p}_{A'_1} + \hat{p}_{B_1})/\sqrt{2}$ and $\hat{x}_D = (\hat{x}_{A'_1} - \hat{x}_{B_1})/\sqrt{2}$, respectively. The measurement results are fed forward to the the remaining modes $\hat{B}_2, \hat{B}_3$ through classical channels. The output beams are

$$\hat{B}'_2 = \hat{B}_3 + \sqrt{2}g\,\hat{x}_D + i\sqrt{2}g\,\hat{p}_C,$$
$$\hat{B}'_3 = \hat{B}_3 + \sqrt{2}g\,\hat{x}_D, \qquad (9)$$

where g is the gain factor in classical channels. Finally, a four-mode state consisting of $\hat{A}_3$, $\hat{A}_2$, $\hat{B}'_2$, and $\hat{B}'_3$ is established, and the EPR steering of output modes is verified.
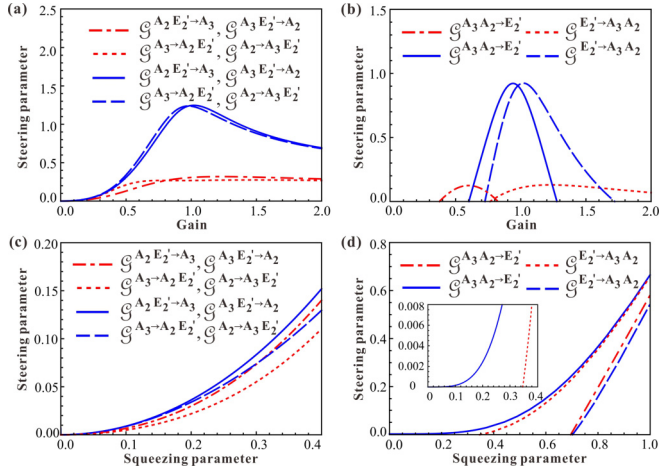
FIG. 2. Dependence of steering parameter between one and the other two modes on the gain factor and squeezing parameter in steering swapping scheme I. (a), (b) Dependence of steering parameter between one and the other two modes on gain factor with two different squeezing parameters. Red dashed-dotted and dotted lines represent $r = 0.57$, blue solid and dashed lines represent $r = 1.15$. (c), (d) Dependence of EPR-steering parameter between one and the remaining two modes on squeezing parameter with unit gain (red dashed-dotted and dotted lines) and optimal gain (blue solid and dashed lines), respectively.

III. RESULTS AND DISCUSSION

A. Results of steering swapping scheme I

The EPR steering after the swapping operation depends on the gain factors in the classical channels. The optimal gain factor reduces the demand for the initial squeezing at the maximal extent [32]. Since there are different types of EPR steering for a multipartite state, it is impossible to optimize all types of EPR steering after the swapping operation with an optimal gain factor. Considering that different quantum communication protocols rely on different types of EPR steering, we can optimize the corresponding EPR steering we need for the quantum communication protocol in the swapping operation. So, the following EPR steering parameters are obtained with the corresponding optimal gain factor in the classical channels.

Figures 2(a) and 2(b) show the dependence of the steering parameter between one and two modes on the gain factor g in steering swapping scheme I when unit transmission efficiency is chosen (lossless channel). The steering parameters with the two squeezing parameters 0.57 (red dashed-dotted and dotted lines) and 1.15 (blue solid and dashed lines) are presented. As the squeezing parameter increases, the optimal gain factors for $\mathcal{G}^{A_3 \to A_2 E_2'}$ ($\mathcal{G}^{A_2 \to A_3 E_2'}$) and $\mathcal{G}^{A_2 E_2' \to A_3}$ ($\mathcal{G}^{A_3 E_2' \to A_2}$) tend to 1 from opposite direction, and steerabilities also substantially increase. Thus $g = 1$ corresponds to the ideal swapping operation in the limit of infinite squeezing.

In the QSS protocol based on EPR steering, the collective steerability of one mode $\{k_1\}$ by group modes $\{k_2, \dots, k_m\}$ provides basis for QSS. Figure 2(c) and 2(d) show the dependence of steering parameters on the squeezing parameter r with unit gain (red dashed-dotted and dotted lines) and

the optimal gain (blue solid and dashed lines). Figure 2(c) shows that EPR steerabilities between mode $\hat{A}_3$ ($\hat{A}_2$) and the other modes with optimal gain factor $g_{\text{opt}}^{A_2 E_2' \to A_3}$ ($g_{\text{opt}}^{A_3 E_2' \to A_2}$) (blue solid and dashed lines) are higher than those with the unit gain (red dashed-dotted and dotted lines). As shown in Fig. 2(d), when unit gain is chosen, EPR steerabilities $\mathcal{G}^{A_3 A_2 \to E_2'}$ and $\mathcal{G}^{E_2' \to A_3 A_2}$ exist only when r is larger than 0.695 and 0.346, respectively (red dashed-dotted and dotted lines). One-way steering $\mathcal{G}^{E_2' \to A_3 A_2}$ is observed in the range of $0.346 < r < 0.695$. So, in our analysis, we optimize the collective steerability by choosing optimal gain factors in the classical channel. When the optimal gain $g_{\text{opt}}^{A_3 A_2 \to E_2'}$ is chosen, EPR steerability of $\mathcal{G}^{A_3 A_2 \to E_2'}$ is obtained with nonzero squeezing (blue solid line), i.e., the requirement of the squeezing parameter is reduced. Please note that although the optical mode is not transmitted over a lossy channel in this case, one-way steering is also presented. This is because the symmetry of the output state is broken after the swapping process, just as the previously observed one-way EPR steering in a lossy channel [23].

Comparing the EPR steerability $\mathcal{G}^{A_3 A_2 \to E_2'}$ with unit gain and optimal gain $g_{\text{opt}}^{A_3 A_2 \to E_2'}$, the required squeezing parameter for $\mathcal{G}^{A_3 A_2 \to E_2'}$ is reduced from 0.695 to 0 with optimal gain $g_{\text{opt}}^{A_3 A_2 \to E_2'}$. However, the required squeezing parameter for $\mathcal{G}^{E_2' \to A_3 A_2}$ is increased from 0.346 to 0.703 by choosing the optimal gain $g_{\text{opt}}^{A_3 A_2 \to E_2'}$. This is because the optimal gain $g_{\text{opt}}^{A_3 A_2 \to E_2'}$ is used to maximize the EPR steerability $\mathcal{G}^{A_3 A_3 \to E_2'}$. If the optimal gain factor $g_{\text{opt}}^{E_2' \to A_3 A_2}$ is chosen, the required squeezing parameter for $\mathcal{G}^{E_2' \to A_3 A_2}$ will be reduced while the requirement of the squeezing parameter for $\mathcal{G}^{A_3 A_2 \to E_2'}$ will be increased. The reason for this phenomenon comes from the asymmetric property of EPR steering.

Figure 3 shows the quantum steering parameters in steering swapping scheme I in a lossy channel, where the squeezing parameter $r = 1.15$ (corresponding to 10 dB squeezing) is chosen. The EPR steering between any two modes does not exist after steering swapping [Fig. 3(a)]. The physical reason is that the quantum steering of the tripartite GHZ state allows no pairwise bipartite steering between any of the three modes in the GHZ state [36,46], which means that two distinct modes cannot steer a third mode simultaneously by Gaussian measurements. In fact, modes $\hat{A}_3$ and $\hat{A}_2$ are completely symmetric in the original GHZ state. Thus, if one mode could be steered by $\hat{A}_3$, it should be equally steered by $\hat{A}_2$ too, which, on the contrary, is forbidden by the monogamy relation.

Figure 3(b) shows the dependence of EPR steering between one and the other two modes on transmission efficiency in a lossy channel, where the squeezing parameter $r = 1.15$ is chosen. The optimal gain factor that optimizes the collective steerability between two modes $\{\hat{i}, \hat{j}\}$ and the other mode $\{\hat{k}\}$ is chosen as an example. It is common and comprehensible that the steerability is reduced with the decrease of transmission efficiency. The red dashed-dotted and dotted lines show the EPR steering $\mathcal{G}^{A_2 E_2' \to A_3}$ ($\mathcal{G}^{A_3 E_2' \to A_2}$) and $\mathcal{G}^{A_3 \to A_2 E_2'}$ ($\mathcal{G}^{A_2 \to A_3 E_2'}$) always exist when the optimal gain factor $g_{\text{opt}}^{A_2 E_2' \to A_3}$ is chosen. The blue solid and dashed lines show the steering parameter between mode $\hat{E}_2'$ and the other modes. When the optimal

FIG. 4. EPR-steering parameter between any two modes for the steering swapping scheme II. The black dashed-dotted line represents the situation that the steering does not exist. The red dashed-dotted and dotted lines represent the steering parameter when the optimal gain factor $g_{\mathrm{opt}}^{B_3' \to B_2'}$ is chosen.
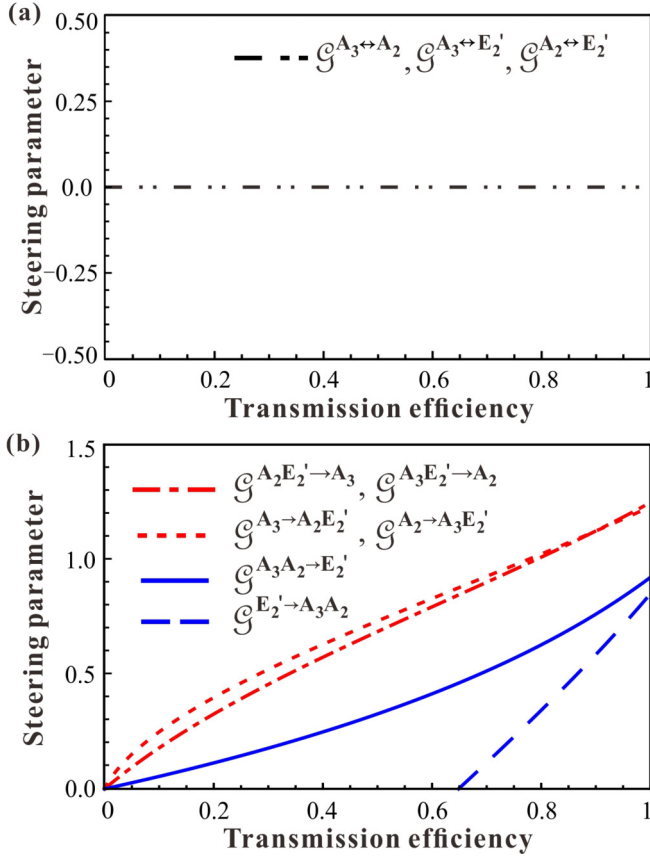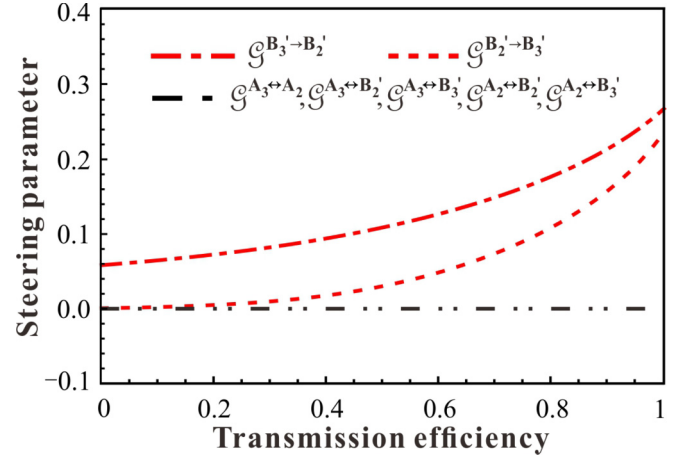

FIG. 3. Dependence of EPR-steering parameter in steering swapping scheme I on transmission efficiency. (a) There is no EPR steering between any two modes of output modes (black dashed-dotted line). (b) EPR-steering parameter between one and the other two modes of output modes. Red dashed-dotted and dotted lines represent the situation where one mode is located in network A. Blue solid and dashed lines correspond to the situation where one mode is located in network B.
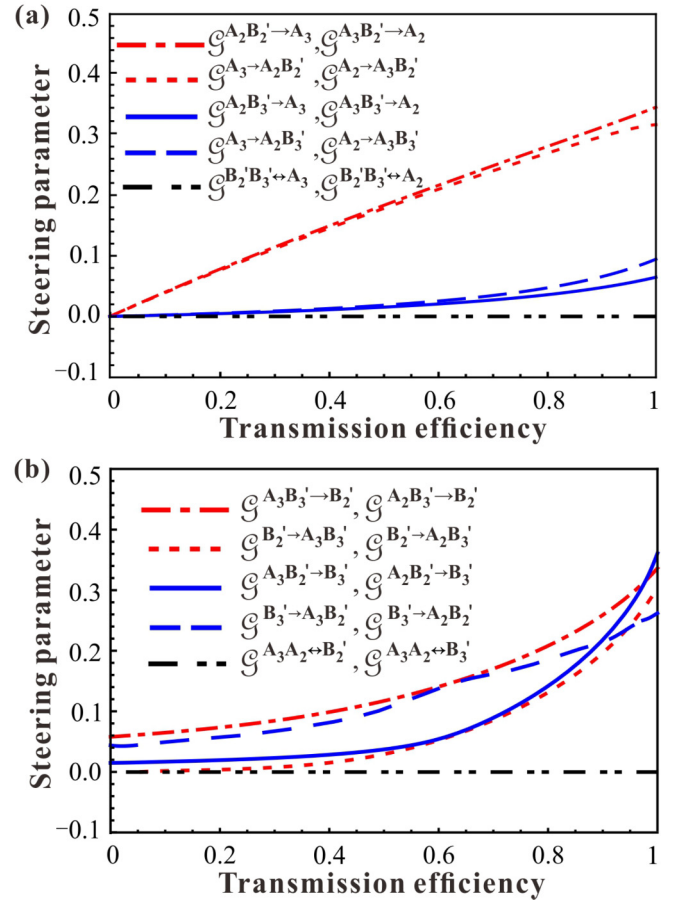

FIG. 5. Dependence of EPR steering on the transmission efficiency between one and the other two modes in swapping scheme II. (a) Dependence of steerabilities between one mode located in network A and the other two modes of the output state. (b) Dependence of steerabilities between one mode located in network B and the other two modes of the output state.

gain factor $g_{\mathrm{opt}}^{A_3 A_2 \to E_2'}$ is chosen, the steering $\mathcal{G}^{A_3 A_2 \to E_2'}$ always exists and the steering $\mathcal{G}^{E_2' \to A_3 A_2}$ can be obtained when the transmission efficiency is higher than 0.649 (blue dashed line). One-way steering $\mathcal{G}^{A_3 A_2 \to E_2'}$ is observed in the range of $0 < T < 0.649$ in a lossy channel. It is obvious that the three-party QSS can be implemented based on these collective steerabilities among modes $\hat{A}_2$, $\hat{A}_3$, and $\hat{E}_2'$ belonging to two local networks.

B. Results of steering swapping scheme II

In the steering swapping scheme II, a four-mode state is obtained after the swapping operation. Various types of EPR steering are observed for the obtained four-mode state. The dependence of EPR steering on transmission efficiency are shown in Figs. 4–7 when the optimal gain factors and squeezing parameter $r = 1.15$ (corresponding to 10 dB squeezing) are chosen.

Figure 4 shows the dependence of the EPR steering between any two modes. The black dashed-dotted line represents that EPR steering between two modes does not exist. Different
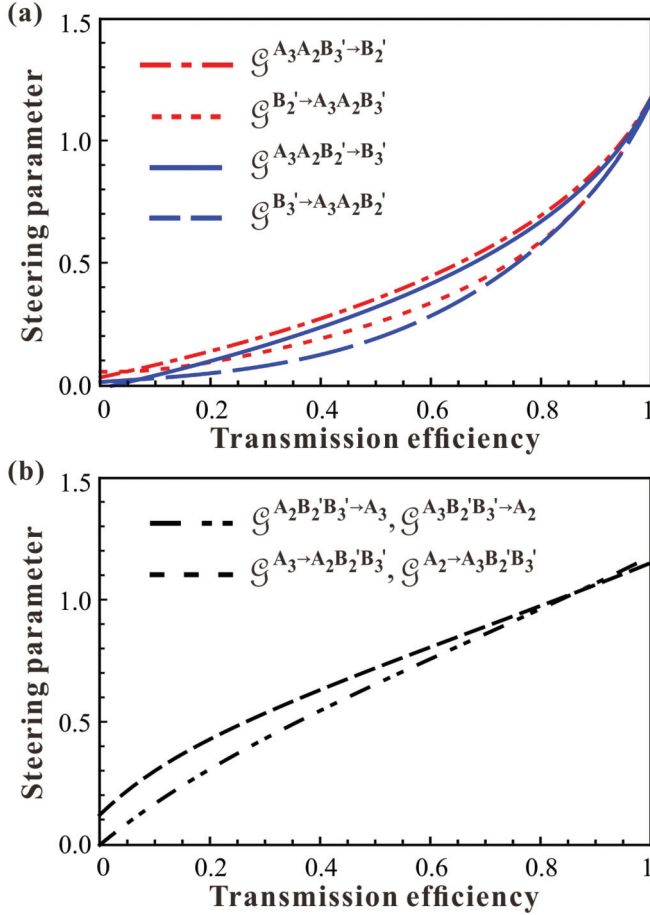
FIG. 6. (a) Dependence of EPR-steering parameter on the transmission efficiency between one mode located in network B and the remaining three modes. Red dashed-dotted and dotted lines represent the EPR steering between $\hat{B}_2'$ and the remaining three modes. Blue dashed-dotted and dotted lines represent the EPR steering between $\hat{B}_3'$ and the remaining three modes. (b) Dependence of EPR steering between the one mode located in network A and the remaining three modes on the transmission efficiency.
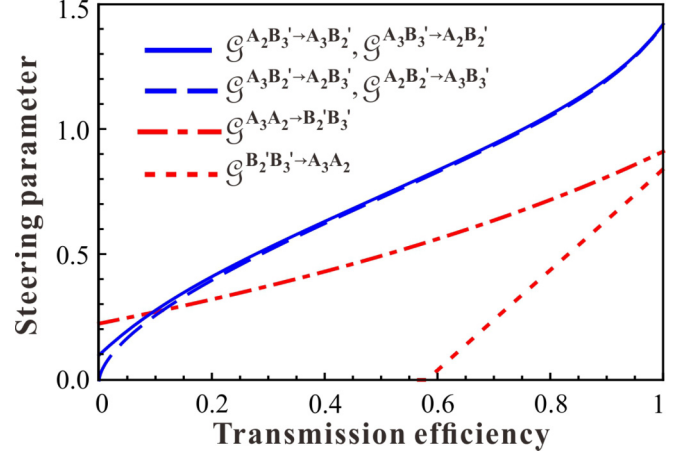

FIG. 7. Dependence of EPR steering parameter on the transmission efficiency between two modes and the remaining two modes. Red dashed-dotted and dotted lines represent the EPR steering between two modes located in one local network and the remaining two modes. Blue solid and dashed lines represent the EPR steering between two modes located in two local networks and the remaining two modes.

from scheme I, we find that pairwise bipartite steering between modes $\hat{B}_2'$ and $\hat{B}_3'$ exists when the optimal gain factor $g_{\mathrm{opt}}^{B_3' \to B_2'}$ is chosen, although the pairwise steering does not exist in the original tripartite GHZ entangled state.

The collective steerabilities between two modes $\{\hat{\imath}, \hat{\jmath}\}$ and another mode $\{\hat{k}\}$, which can be used to implement QSS for three parties, are shown in Fig. 5. Figure 5(a) shows the dependence of steerabilities between the one mode located in network A and any other two modes of the output state. The red dashed-dotted and dotted lines (blue solid and dotted lines) are the steerability between modes $\hat{A}_3$ and $\hat{A}_2\hat{B}_2'$ ($\hat{A}_2\hat{B}_3'$) when the optimal gain $g_{\mathrm{opt}}^{A_2 B_2' \to A_3}$ ($g_{\mathrm{opt}}^{A_2 B_3' \to A_3}$) is chosen as an example. The EPR steering only exists between mode $\hat{A}_3$ ($\hat{A}_2$) and a group comprising the mode $\hat{A}_2$ ($\hat{A}_3$) ($\mathcal{G}^{A_3 \to A_2 B_2'} = \mathcal{G}^{A_2 \to A_3 B_2'} > 0$, $\mathcal{G}^{A_2 B_2' \to A_3} = \mathcal{G}^{A_3 B_2' \to A_2} > 0$, $\mathcal{G}^{A_3 \to A_2 B_3'} = \mathcal{G}^{A_2 \to A_3 B_3'} > 0$, $\mathcal{G}^{A_2 B_3' \to A_3} = \mathcal{G}^{A_3 B_3' \to A_2} > 0$). This means that the QSS can be implemented when the two players are separated in two local quantum networks and collaborate to

decode the secret sent by the dealer who owns the other mode located in local quantum network A.

Figure 5(b) shows the steerabilities between the one mode located in network B and any other two modes of the output state. We can see that the EPR steering only exists between mode $\hat{B}_2'$ ($\hat{B}_3'$) and a group comprising the mode $\hat{B}_3'$ ($\hat{B}_2'$). The EPR steering $\mathcal{G}^{A_3 B_3' \to B_2'}$ ($\mathcal{G}^{A_2 B_3' \to B_2'}$) and $\mathcal{G}^{B_2' \to A_3 B_3'}$ ($\mathcal{G}^{B_2' \to A_2 B_3'}$) exist with optimal gain factor $g_{\mathrm{opt}}^{A_3 B_3' \to B_2'}$ ($g_{\mathrm{opt}}^{A_3 B_2' \to B_3'}$) when the transmission efficiency is larger than 0 and 0.056 (red dashed-dotted and dotted lines). We have to point out that the potential security risk may exist for three-party QSS when the dealer is located in local quantum network B, due to the existence of EPR steering between $\hat{B}_2'$ and $\hat{B}_3'$, as shown in Fig. 4.

We also find that EPR steering $\mathcal{G}^{B_2' B_3' \leftrightarrow A_2}$, $\mathcal{G}^{B_2' B_3' \leftrightarrow A_3}$, $\mathcal{G}^{A_2 A_3 \leftrightarrow B_2'}$, and $\mathcal{G}^{A_2 A_3 \leftrightarrow B_3'}$ (the black dashed-dotted line in Fig. 5) does not exist even if the optimal gain factors are chosen. This means that the three-party QSS cannot be implemented when the dealer owns one mode that is in a local quantum network and another two players are in another local quantum network.

Figure 6 shows the dependence of EPR steering between one and the other three modes on transmission efficiency of the quantum channel. Figure 6(a) represents the steering parameters when the one mode (one party) is located in network B. The EPR steering between $\hat{B}_2'$ ($\hat{B}_3'$) and the other three modes with the optimal gain factor $g_{\mathrm{opt}}^{A_3 A_2 B_3' \to B_2'}$ ($g_{\mathrm{opt}}^{A_3 A_2 B_2' \to B_3'}$) exists. As shown in Fig. 6(b), when the one mode is located in network A, the quantum steering $\mathcal{G}^{A_3 \to A_2 B_2' B_3'}$ ($\mathcal{G}^{A_2 \to A_3 B_2' B_3'}$) and $\mathcal{G}^{A_2 B_2' B_3' \to A_3}$ ($\mathcal{G}^{A_3 B_2' B_3' \to A_2}$) always exist with the optimal gain factor $g_{\mathrm{opt}}^{A_2 B_2' B_3' \to A_3}$ (black dashed-dotted and dotted lines). This type of EPR steering can be used to implement the QSS for four parties when the dealer is located in the local quantum network A. Considering the existence of EPR steering between $\hat{B}_2'$ and $\hat{B}_3'$, the potential security risk may exist for four-party QSS when the dealer is located in network B.

Finally, we analyze the Gaussian EPR steering parameters between two modes and the other two modes in a lossy quantum channel, which are shown in Fig. 7. When the optimal gain $g_{\text{opt}}^{A_3 A_2 \rightarrow B_2' B_3'}$ is chosen, one-way steering $\mathcal{G}^{A_3 A_2 \rightarrow B_2' B_3'}$ is observed, where two modes $\hat{A}_3$ and $\hat{A}_2$ can always steer the remaining two modes $\hat{B}_2'$ and $\hat{B}_3'$, but $\hat{B}_2'$ and $\hat{B}_3'$ only steer $\hat{A}_3$ and $\hat{A}_2$ when the transmission efficiency is higher than 0.534 (red dotted line). The blue solid and dashed lines show that the two-way steering $\mathcal{G}^{A_2 B_3' \rightarrow A_3 B_2'}$ ($\mathcal{G}^{A_3 B_3' \rightarrow A_2 B_2'}$) and $\mathcal{G}^{A_3 B_2' \rightarrow A_2 B_3'}$ ($\mathcal{G}^{A_2 B_2' \rightarrow A_3 B_3'}$) always exists with the optimal gain $g_{\text{opt}}^{A_2 B_3' \rightarrow A_3 B_2'}$.

IV. CONCLUSION

In conclusion, EPR-steering swapping between two Gaussian multipartite entangled states is presented. Two specific steering swapping schemes, including swapping between a tripartite GHZ state and an EPR state and that between two tripartite GHZ states, are discussed as examples. Various types of EPR steering are observed for the output states of the swapping schemes. Based on the covariance matrix of the output state, we obtain a full steering characterization for all bipartite configurations with arbitrary number of modes in each side. The optimal gain factors are used to optimize the obtained EPR steering in the calculation. Different from entanglement swapping, the obtained steerabilities of the two parties and the dependence on the squeezing parameter are different in two directions due to the asymmetric property, and the one-way property can be observed.

For the swapping scheme between a tripartite GHZ state and an EPR state, there is no steerability between any two modes and only the collective steerabilities between two and one modes are observed, which is a perfect resource for three-party QSS. For the swapping scheme between two tripartite GHZ states, various types of EPR steering are presented, where three- and four-party QSSs can be implemented based on corresponding EPR steering. In principle, this method may also be extended to construct large-scale multipartite EPR steering states, which are very useful for quantum computation networks and secure teleportation. Of course, the feed-forward scheme is important and needs to be designed according to different correlation requirements.

[1] X. Su, C. Tian, X. Deng, Q. Li, C. Xie, and K. Peng, Phys. Rev. Lett. **117**, 240503 (2016).

[2] C. H. Bennett, G. Brassard, C. Crépeau, R. Jozsa, A. Peres, and W. K. Wootters, Phys. Rev. Lett. **70**, 1895 (1993).

[3] M. Zukowski, A. Zeilinger, M. A. Horne, and A. K. Ekert, Phys. Rev. Lett. **71**, 4287 (1993).

[4] R. E. S. Polkinghorne and T. C. Ralph, Phys. Rev. Lett. **83**, 2095 (1999).

[5] S. M. Tan, Phys. Rev. A **60**, 2752 (1999).

[6] P. van Loock and S. L. Braunstein, Phys. Rev. A **61**, 010302(R) (1999).

[7] J. Zhang, C. Xie, and K. Peng, Phys. Lett. A **299**, 427 (2002).

[8] H.-J. Briegel, W. Dur, J. I. Cirac, and P. Zoller, Phys. Rev. Lett. **81**, 5932 (1998).

[9] L.-M. Duan, M. D. Lukin, J. I. Cirac, and P. Zoller, Nature **414**, 413 (2001).

[10] J.-W. Pan, D. Bouwmeester, H. Weinfurter, and A. Zeilinger, Phys. Rev. Lett. **80**, 3891 (1998).

[11] X. Jia, X. Su, Q. Pan, J. Gao, C. Xie, and K. Peng, Phys. Rev. Lett. **93**, 250503 (2004).

[12] S. Takeda, M. Fuwa, P. van Loock, and A. Furusawa, Phys. Rev. Lett. **114**, 100501 (2015).

[13] C.-Y. Lu, T. Yang, and J.-W. Pan, Phys. Rev. Lett. **103**, 020501 (2009).

[14] L. Ma and X. Su, Opt. Express **22**, 15894 (2014).

[15] A. Einstein, B. Podolsky, and N. Rosen, Phys. Rev. **47**, 777 (1935).

[16] E. Schrödinger, Proc. Cambridge Philos. Soc. **31**, 555 (1935).

[17] E. Schrödinger, Proc. Cambridge Philos. Soc. **32**, 446 (1936).

[18] J. S. Bell, Physics **1**, 195 (1964).

[19] R. Horodecki, P. Horodecki, M. Horodecki, and K. Horodecki, Rev. Mod. Phys. **81**, 865 (2009).

[20] H. M. Wiseman, S. J. Jones, and A. C. Doherty, Phys. Rev. Lett. **98**, 140402 (2007).

[21] S. J. Jones, H. M. Wiseman, and A. C. Doherty, Phys. Rev. A **76**, 052116 (2007).

[22] P. Skrzypczyk, M. Navascués, and D. Cavalcanti, Phys. Rev. Lett. **112**, 180404 (2014).

[23] V. Händchen, T. Eberle, S. Steinlechner, A. Samblowski, T. Franz, R. F. Werner, and R. Schnabel, Nat. Photonics **6**, 596 (2012).

[24] S. Armstrong, M. Wang, R. Y. Teh, Q. H. Gong, Q. Y. He, J. Janousek, H. A. Bachor, M. D. Reid, and P. K. Lam, Nat. Phys. **11**, 167 (2015).

[25] S. Wollmann, N. Walk, A. J. Bennet, H. M. Wiseman, and G. J. Pryde, Phys. Rev. Lett. **116**, 160403 (2016).

[26] K. Sun, X. J. Ye, J. S. Xu, X. Y. Xu, J. S. Tang, Y. C. Wu, J. L. Chen, C. F. Li, and G. C. Guo, Phys. Rev. Lett. **116**, 160404 (2016).

[27] C. Branciard, E. G. Cavalcanti, S. P. Walborn, V. Scarani, and H. M. Wiseman, Phys. Rev. A **85**, 010301 (2012).

[28] Y. Xiang, I. Kogias, G. Adesso, and Q. He, Phys. Rev. A **95**, 010101(R) (2017).

[29] M. Piani and J. Watrous, Phys. Rev. Lett. **114**, 060404 (2015).

[30] M. D. Reid, Phys. Rev. A **88**, 062338 (2013).

[31] Q. He, L. Rosales-Zárate, G. Adesso, and M. D. Reid, Phys. Rev. Lett. **115**, 180502 (2015).

[32] M. Wang, Z. Qin, and X. Su, Phys. Rev. A **95**, 052311 (2017).

[33] Z. Qin, X. Deng, C. Tian, M. Wang, X. Su, C. Xie, and K. Peng, Phys. Rev. A **95**, 052114 (2017).

[34] D. Cavalcanti, P. Skrzypczyk, G. H. Aguilar, R. V. Nery, P. H. Souto Ribeiro, and S. P. Walborn, Nat. Commun. **6**, 7941 (2015).

[35] C.-M. Li, K. Chen, Y.-N. Chen, Q. Zhang, Y.-A. Chen, and J.-W. Pan, Phys. Rev. Lett. **115**, 010402 (2015).

[36] M. D. Reid, Phys. Rev. A **88**, 062108 (2013).

[37] S.-W. Ji, M. S. Kim, and H. Nha, J. Phys. A: Math. Theor. **48**, 135301 (2015).

[38] G. Adesso and R. Simon, J. Phys. A: Math. Theor. **49**, 34LT02 (2016).

[39] L. Lami, C. Hirche, G. Adesso, and A. Winter, Phys. Rev. Lett. **117**, 220502 (2016).

[40] X. Deng, Y. Xiang, C. Tian, G. Adesso, Q. He, Q. Gong, X. Su, C. Xie, and K. Peng, Phys. Rev. Lett. **118**, 230501 (2017).

[41] A. Shamir, Commun. ACM **22**, 612 (1979).

[42] H. J. Kimble, Nature (London) **453**, 1023 (2008).

[43] I. Kogias, A. R. Lee, S. Ragy, and G. Adesso, Phys. Rev. Lett. **114**, 060403 (2015).

[44] X. Deng, S. Hao, C. Tian, X. Su, C. Xie, and K. Peng, Appl. Phys. Lett. **108**, 081105 (2016).

[45] X. Su, Chin. Phys. B **22**, 080304 (2013).

[46] V. Coffman, J. Kundu, and W. K. Wootters, Phys. Rev. A **61**, 052306 (2000).